750 KEV BEAM LINE CONSTRUCTION AT THE KEK

H. Ishimaru, S. Anami, T. Inagaki, T. Sakaue, K. Itoh and S. Fukumoto
National Laboratory for High Energy Physics
Oho-machi, Tsukuba-gun, Ibaraki, 300-32, Japan

Abstract

The construction of 750 keV beam line of the KEK injector of the 12 GeV proton synchrotron was described. The beam line consists of the beam focusing quadrupoles, vacuum system, the electrostatic chopper and the various beam monitors.

Introduction

Started in September, 1972, the construction of 750 keV beam line of KEK injector of the 12 GeV proton synchrotron had been constructed. First 750 keV proton beam had been transported from column to a linac on 24 July 1974. Efforts are continued to improve the beam characteristics and the various monitor system.

Beam Trajectories and Focusing System

The basic design[1] is somewhat modified after calculations of ion beam optics. Assuming the emittance of the ion source and the acceptance of the linac as shown in Fig.1, the beam envelopes are calculated by the program LINDA.[2] The first matching section composed of a quadruplet and a triplet is enclosed, just after the accelerating gap, in the column.[3] A steering magnet system is inserted between the quadruplet and the triplet. Between first matching section and the linac, there are four triplets. The last two triplets compose the second matching section. The calculated beam envelopes are shown in Fig.2. The quadrupole magnets parameters are shown in Table I. The length of the transport line is 7 m.

Quadrupole Magnets and Steering Magnets

The maximum field gradient of the quadrupole magnets is 1.9 kgauss/cm. The maximum field of the steering magnets is 240 gauss. Both magnets are excited by dc power sources. The dimensions of the quadrupole magnet are determined by the results of calculations of field distribution in the pole, yoke and the field gradient uniformity versus the radius of the pole tips. The calculated field distribution in the pole and the yoke is shown in Fig.3.

The calculated field gradient of the quadrupole magnet versus the radius of the pole tip is shown in Fig.4. The radius of the pole tip is chosen to be $1.17\ r_0$, where r_0 is a bore radius of the quadrupole magnet. The parameters of the mechanical and electrical design of quadrupole magnets are shown in Table II. Also the parameters of the mechanical and electrical design of the steering magnets are shown in Table III.

The measurement of the field gradient was carried out by the vibrating coil method. A schematic diagram for the field gradient measurement is shown in Fig.5. The accuracy of the measurement is better than 10^{-3}.

Uniformity of the radial component of the measured field gradient is $2\sim3 \times 10^{-3}$ up to about 70% aparture as shown in Fig.6. Axial component of the measured field gradient is shown in Fig.7. DC power sources for exciting the quadrupole magnets and the steering magnets are stabilized within the order of 10^{-4}. Quadrupole magnets can be divided into two parts, for convenience of aligning of the magnets and setting of the beam ducts. A photograph of the quadrupole magnet is shown in Fig.8. The winding of the coils is about 10 layer of the enamel wire with cross section of 2.2×1.8 mm. The cooling pipe of 10×5 mm cross section is wound for single layer on the outside of the coil. These coil and the cooling layer filled with epoxy resin in vacuum and cured in a thermostatic oven.

Vacuum System

Since clean or oil free vacuum is necessary for the high gradient accelerating column the turbomolecular pump and the sputter ion pumps are preferably used. As the hydrogen gas consumption of the duoplasmatron is about 0.2 torr ℓ/sec, a 650 ℓ/sec turbomolecular pump is mainly in $2\sim3 \times 10^{-4}$ torr. Sputter ion pumps are only used to preserve the high vacuum without beam. The length of the accelerating column and the beam duct is about 8.5 m and the total system volume is about 3000 ℓ. The wall thickness of the beam ducts is about 2 mm, the material is stainless steel SUS-304. Flanges jointed with Viton O-ring gaskets are used. Various chemical cleaning and glass bead blast cleaning are performed to reduce surface out-gassing rates. A forevacuum pump is a combination of the rotary pump and mechanical booster pump. A diagram of the vacuum system is shown in Fig.9. The vacuum pressures are monitored by 1 ℓ/sec appendage ion pumps at two positions. The pressure along the beam from the accelerating gap to the linac is so high that the space charge effect may be reduced by trapping of the secondary electron for gas ionization process.

Electrostatic Chopper

Since the beam from the ion source does not rise and fall so quickly, the beam is chopped by pulsed electric field. The pulse length of the chopped beam is variable from 0.6 μsec to 20 μsec. Its rise and fall times are 100 nsec. As 0.6 μsec corresponds to the one turn time of the beam injected into the 500 MeV booster, the thin beam is useful for surveying the various machine tuning study, while the long beam is used for multi-turn injection.

A schematic diagram of the electrostatic chopper is shown in Fig.10. The chopper consists of two 200 mm in diameter plates separated by 40 mm. The high voltage pulse generator is connected to electrodes with coaxial vacuum tight feedthrough and short coaxial feeder. The stray capacitance of the high voltage side including the electrodes is about 40 pF. The output double pulses is shown in Fig.11. The deflected ion beam is intercepted by water cooled collimator as shown in Fig.12.

Collimator and Beam Shutter

There are two collimators. The first one whose diameter is 30 mm is placed upstream of the electrostatic chopper avoiding the beam from hitting the chopper electrodes. The second collimator, with three fixed apertures whose diameters are 10, 20, 30 mm respectively, driven by stepping motor is installed. The variable aperture collimator is shown in Fig.12. The small apertures are used for making pencil-beams, which is very convenient for tuning not only the linear accelerator, but also the booster and the main synchrotron.

The fast acting beam shutter for emergency is also installed. This shutter is moved by pneumatic valve which is installed in vacuum chamber.

Buncher

Single buncher is equipped. The buncher is a coaxial cavity type. The bore is 40 mm in diameter and some tungsten grids are attached to make the electric field uniform. The buncher is installed in front of the last triplet, 800 mm upstream of the linac.

Beam Monitors and Control System

A number of diagnostic devices have been built and used to measure properties of the KEK preinjector beams. The data logging for the focusing system, vacuum system and others is interfaced to mini-computer. The digital printout of the data logging is shown in Fig.13. The control is performed by the KEK standard modules such as an On-Off module, a Up-Down module, a Helipot module, an Interlock module, etc. The pulsed operating equipment are triggered by the master clock pulse with Digital Delay modules.

Setup and Alignment

The optical axis of the ion source, the accelerating column, the quadrupoles and the other equipments are aligned by means of a He-Ne laser. The alignment errors are within about 0.1 mm. Fig.14 shows the schematic diagram of the 750 keV beams line. The bird's-eye view of the 750 keV beam line is shown in Fig.15.

Conclusion

Recently, more than 600 mA ion beam is accelerated, 260 mA is injected into the linac. A 140 mA beam is accelerated to 20 MeV. About 60 % of the current extracted from the ion source is transported to the linac. The advantages of this transport are as follows: 1. It is easy to handle, 2. It has the first quadruplet of large aparture, 3. It has good beam transmission rate after first focusing quadruplet, and the high pressure operation is applied to reduce the space charge effect 4. The axis of the ion source, the accelerating column, the quadrupole and the linac are aligned precisely, so the steering magnets are not used.

We would like to thank Prof. T. Nishikawa for his encouragement.

Reference

1. Th.J.M. Sluyters: KEK 72-1, Jan. 1972
2. J.H. Dorst, UCRL-11798, 1965
3. S. Fukumoto et al, 1976 Proton Linear Accelerato Conference.
4. J.M. Dolique, 1972, International Conf. on Ion Sources , 421
5. H. Ishimaru et al, 1976 Proton Linear Accelerato Conference.

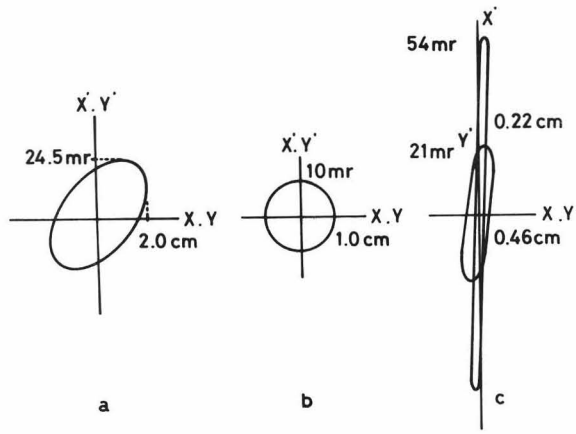

Fig.1 a) Assumed emittance of the ion source,
b) emittance of the π-sections, and
c) acceptance of the linac.

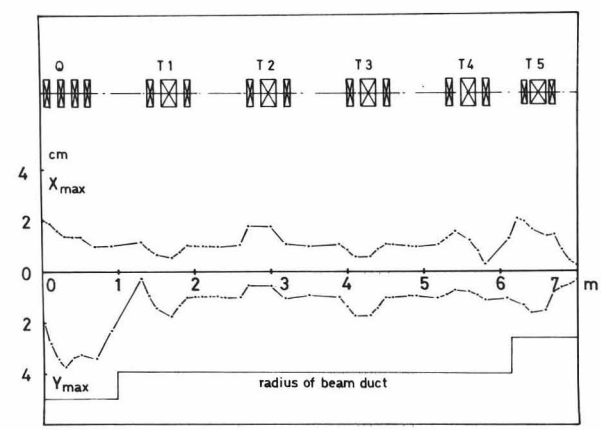

Fig.2 Focusing quadrupoles and calculated beam envelopes.

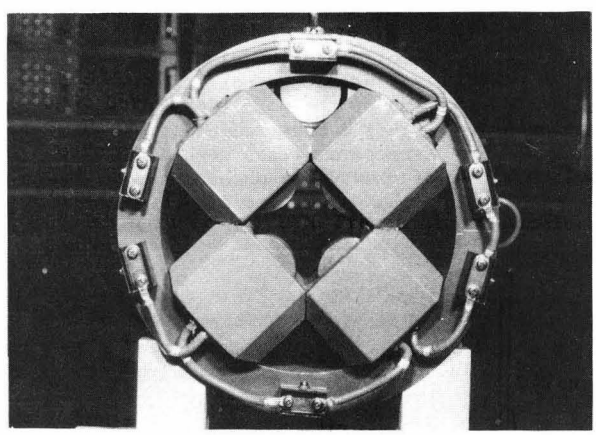

Fig.8 Quadrupole magnet of the 750 keV line.

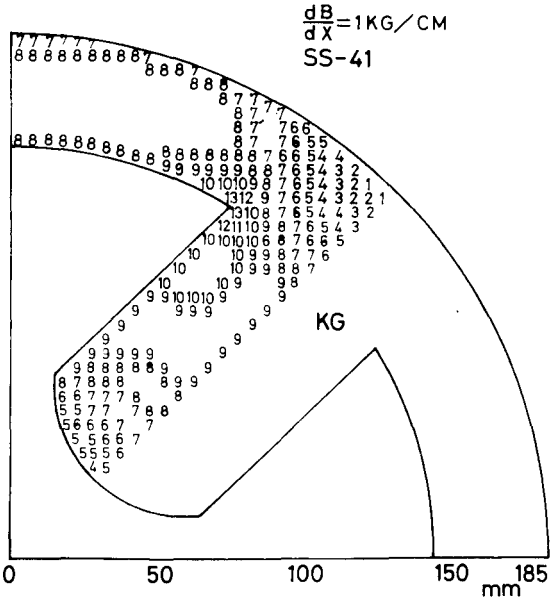

Fig.3 Two-dimensional calculated field distribution in the pole and the yoke.

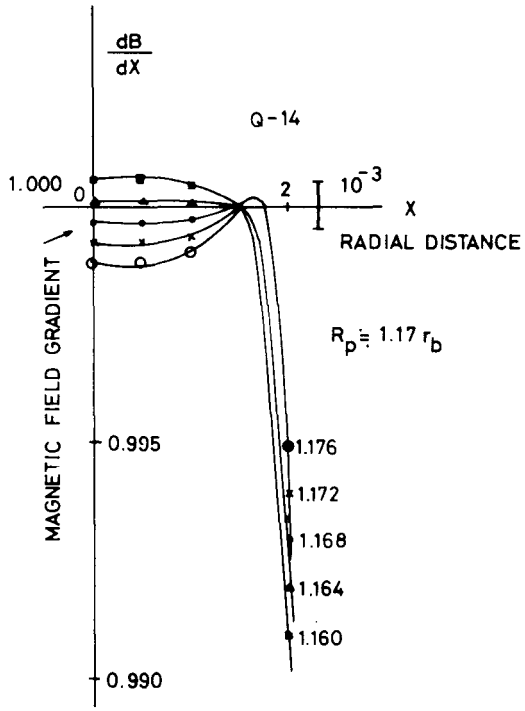

Fig.4 Two-dimensional calculated field gradient v.s. the radius of the pole tips.

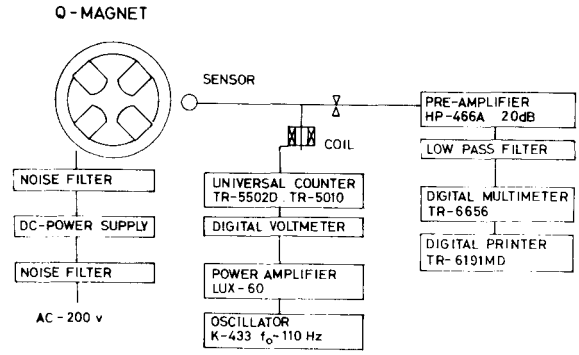

Fig.5 A schematic diagram for the field gradient measurement.

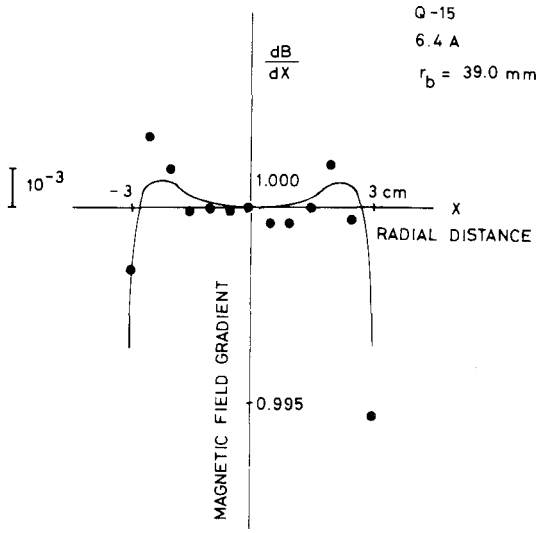

Fig.6 Radial component of the measured field gradient.

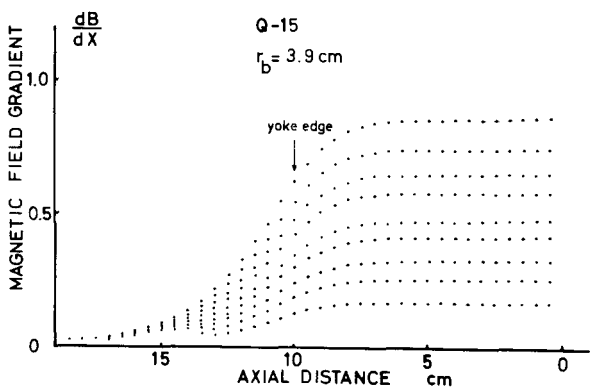

Fig.7 Axial component of the measured field gradient.

	r_0 cm	B_{max} kG	dB/dX kG/cm	X_{max} cm	X'_{max} mr	Y_{max} cm	Y'_{max} mr
				2.00	24.4	2.00	24.4
Q- 1	4.54	1.66	0.366	±1.55	±49.9	±2.86	±109
Q- 2	4.54	-2.07	-0.457	∓1.37	∓16.9	∓3.73	∓62.6
Q- 3	4.54	1.46	0.322	1.35	31.8	3.26	41.5
Q- 4	4.54	-1.23	-0.272	0.994	9.84	3.40	55.3
Q- 5	3.90	1.96	0.503	0.873	46.4	0.950	80.5
Q- 6	3.90	-1.51	-0.389	0.533	43.5	1.73	59.2
Q- 7	3.90	1.96	0.503	1.02	9.86	1.02	9.86
Q- 8	3.90	-1.94	-0.498	1.41	60.8	0.807	43.6
Q- 9	3.90	1.21	0.312	1.78	60.8	0.560	43.6
Q-10	3.90	-1.94	-0.495	1.05	9.86	1.05	9.86
Q-11	3.90	1.94	0.498	0.807	43.6	1.41	60.8
Q-12	3.90	-1.21	-0.312	0.560	43.6	1.78	60.8
Q-13	3.90	1.94	0.498	1.05	9.86	1.05	9.86
Q-14	3.90	-1.24	-0.318	1.30	39.8	0.912	28.4
Q-15	3.90	1.34	0.345	1.18	64.9	0.770	29.3
Q-16	3.90	-1.24	-0.318	0.209	51.9	1.08	9.54
Q-17	2.50	1.95	0.780	1.96	73.7	1.32	67.8
Q-18	2.50	-1.32	-0.528	1.33	35.2	1.51	75.8
Q-19	2.50	1.95	0.780	1.38	54.3	0.786	21.7
				0.214	54.3	0.451	21.7

Table I Quadrupole magnet parameters.

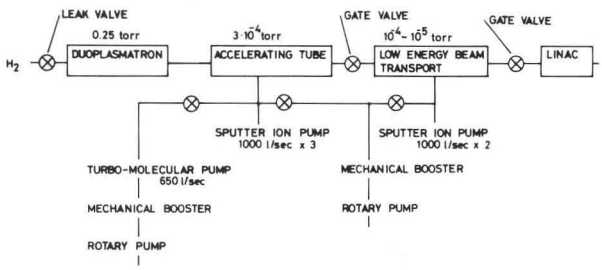

Fig.9 Vacuum system in the ion source, the column and 750 keV beam line.

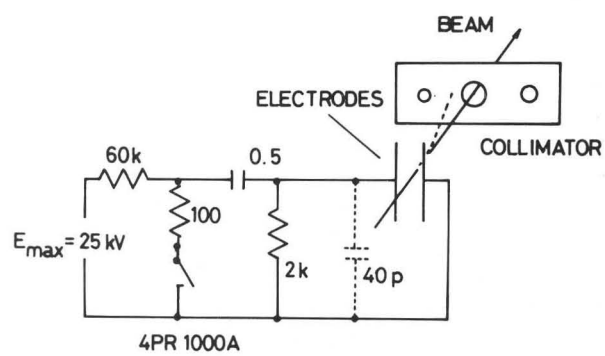

Fig.10 A schematic diagram of the electrostatic chopper.

	r_b mm	R_y mm	L_y mm	T/p	kG/cm	kAT/p	ohm	amp	watts
Q- 1	45.5	185	80	398	0.85	6.84	3.69	16	944
Q- 2	45.5	185	80	398	0.85	6.84	3.69	16	944
Q- 3	45.5	185	80	398	0.85	6.84	3.69	16	944
Q- 4	45.5	185	80	398	0.85	6.84	3.69	16	944
Q- 5	39	185	80	328	0.83	5.24	2.59	16	662
Q- 6	39	185	200	328	0.83	5.24	4.24	16	1084
Q- 7	39	185	80	328	0.83	5.24	2.59	16	662
Q- 8	39	185	80	328	0.83	5.24	2.59	16	662
Q- 9	39	185	200	328	0.83	5.24	4.24	16	1084
Q-10	39	185	80	328	0.83	5.24	2.59	16	662
Q-11	39	185	80	328	0.83	5.24	2.59	16	662
Q-12	39	185	200	328	0.83	5.24	4.24	16	1084
Q-13	39	185	80	328	0.83	5.24	2.59	16	662
Q-14	39	185	80	328	0.83	5.24	2.59	16	662
Q-15	39	185	200	328	0.83	5.24	4.24	16	1084
Q-16	39	185	80	328	0.83	5.24	2.59	16	662
Q-17	25	155	70	290	1.87	4.63	2.04	16	521
Q-18	25	155	165	290	1.87	4.63	2.04	16	816
Q-19	25	155	70	290	1.87	4.63	2.04	16	521

Table II Parameters of the mechanical and electrical design of the quadrupoles. Where r_b is the bore radius, R_y is the radius of the yoke, L_y is the length of the yoke and T/P is the turns of coil per pole.

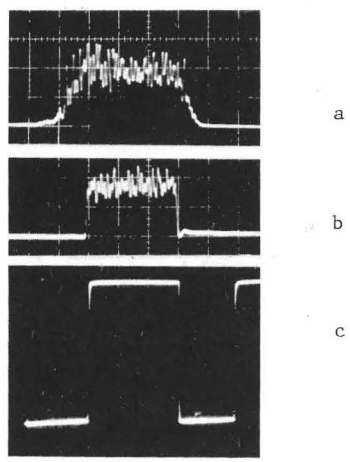

Fig.11 a) Long pulsed ion beam, b) chopped ion beam and c) high voltage double pulse output. Sweep 5 μsec/div.

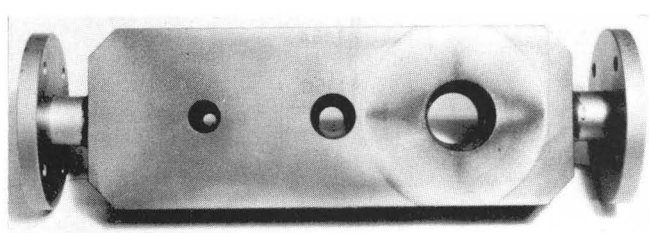

Fig.12 A variable aperture collimator.

max. magnetic field	120 x 2 gauss
max. excitation current	882 x 2 Aturns
turns of winding	210 x 2 turns
current	4.2 A
current density	2.1 A/mm^2
resistance of coil	3.8 ohm
terminal voltage	15.9 x 2 V
power	67 x 2 watts
length of yoke	230 mm
thickness of yoke	20 mm
width of yoke	60 mm

Table III Parameters of the mechanical and electrical design of the steering magnets.

PRE-INJECTOR DATA PRINT OUT DATE 76.06.17 TIME 00:00:11

VACUUM PRESSURE 1	1.87E-04	TORR	LEBT LINAC SIDE	
VACUUM PRESSURE 2	2.48E-04	TORR	ACCEL. COLUMN	
ACCEL.VOLTAGE	754.39	KV		
C. W. CURRENT	1.18	MA		
FIELD COIL CURRENT	2.39	A		
BEAM CURRENT CM-1	598	MA	750 KEV, BEFORE LEBT	
BEAM CURRENT CM-2	341	MA	AFTER STEERINGS	
BEAM CURRENT CM-3	336	MA	COLUMN EXIT	
BEAM CURRENT CM-4	345	MA	BEFORE E. S. CHOPPER	
BEAM CURRENT CM-5	302	MA	AFTER COLLIMATOR	
BEAM CURRENT CM-6	337	MA	BEFORE BUNCHER	
BEAM CURRENT CM-7	255	MA	AFTER BUNCHER, LINAC INPUT	
BEAM CURRENT IM-1	148	UA	LINAC OUTPUT	
Q MAGNET P. S. 1	11.15	A	541.0 GAUSS/CM	QUADRUPLET 1
Q MAGNET P. S. 2	13.43	A	651.7 GAUSS/CM	QUADRUPLET 2
Q MAGNET P. S. 3	12.57	A	610.0 GAUSS/CM	QUADRUPLET 3
Q MAGNET P. S. 4	6.90	A	334.9 GAUSS/CM	QUADRUPLET 4
Q MAGNET P. S. 5	6.29	A	341.2 GAUSS/CM	TRIPLET 1 CENTER
Q MAGNET P. S. 6	6.64	A	359.9 GAUSS/CM	TRIPLET 1 ENDS
Q MAGNET P. S. 7	9.96	A	540.3 GAUSS/CM	TRIPLET 2 ENDS
Q MAGNET P. S. 8	6.54	A	354.8 GAUSS/CM	TRIPLETS 2,3, CENTERS
Q MAGNET P. S. 9	8.35	A	453.0 GAUSS/CM	TRIPLET 3 ENDS
Q MAGNET P. S. 10	6.25	A	338.7 GAUSS/CM	TRIPLET 4 ENDS
Q MAGNET P. S. 12	5.45	A	295.5 GAUSS/CM	TRIPLET 4 CENTER
Q MAGNET P. S. 13	6.29	A	730.4 GAUSS/CM	TRIPLET 5 CENTER
Q MAGNET P. S. 14	11.37	A	1319.5 GAUSS/CM	TRIPLET 5 ENDS
STEERING MAG. X-1	-0.01	A	-0.3 GAUSS	IN COLUMN, HORIZONTAL
STEERING MAG. Y-1	0.00	A	0.0 GAUSS	IN COLUMN, VERTICAL
STEERING MAG. X-2	0.00	A	0.0 GAUSS	IN COLUMN, HORIZONTAL
STEERING MAG. Y-2	-0.01	A	-0.2 GAUSS	IN COLUMN, VERTICAL
ANALOG TEST DATA	-0.0024	V		

Fig. 13 A digital printout of the data logging.

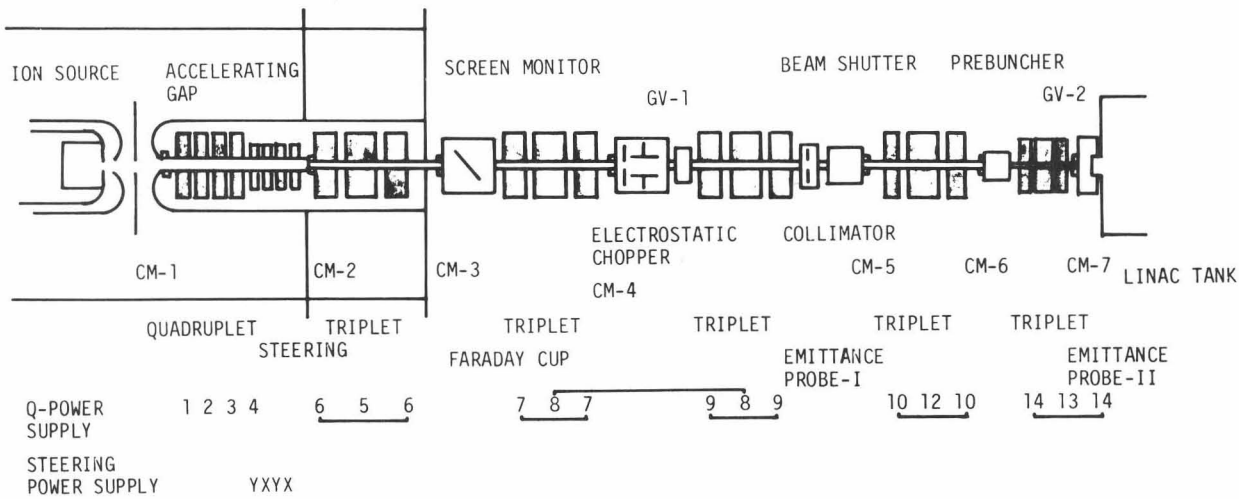

Fig. 14 A schematic diagram of the KEK 750 keV beam line.

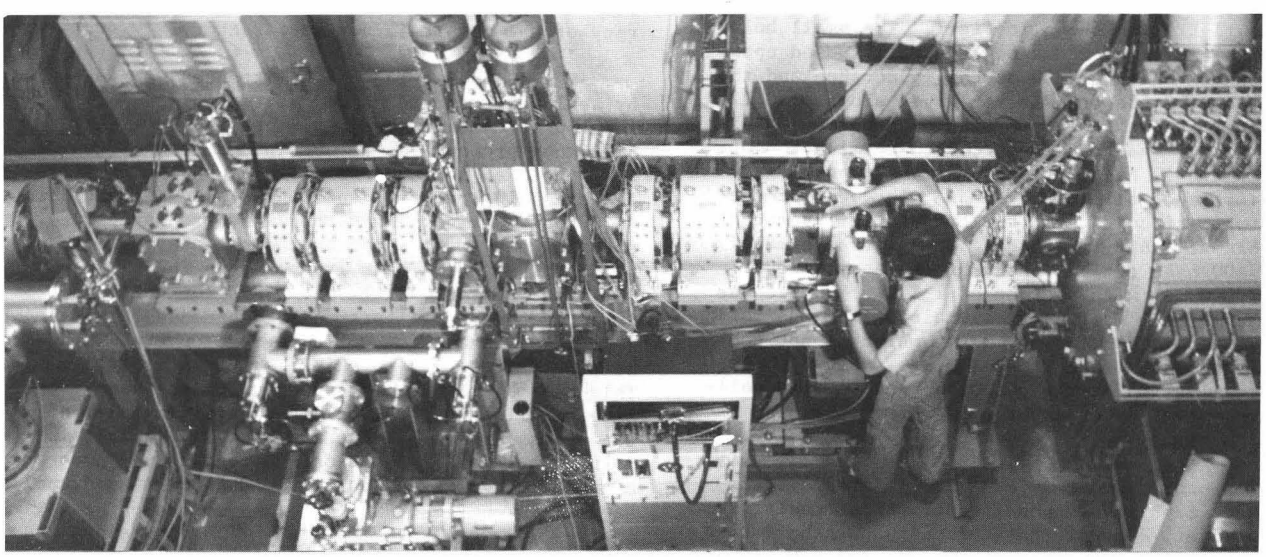

Fig. 15 A bird's-eye view of the 750 keV beam line.